Phonon-associated relaxation of local magnons in FeF_2:Mn

S. M. Rezende
Department of Physics, University of California, Santa Barbara, California 93106
and Departamento de Física, Universidade Federal de Pernambuco, 50000 Recife, Pernambuco, Brazil

D. W. Hone and R. M. Toussaint
Department of Physics, University of California, Santa Barbara, California 93106
(Received 26 September 1983)

The Mn^{2+} impurity-associated mode that lies just below the host spin-wave band in FeF_2 has a residual linewidth (in the limit of very small impurity concentrations, sample dimension, and temperature) in excess of 1 kOe. This value is surprisingly large, since the $k=0$ magnon has a linewidth less than 30 Oe and since the down-going impurity mode is energetically the lowest-lying magnetic excitation in the system. In this paper we analyze several phonon-associated processes that would contribute to the decay of local magnon modes in antiferromagnets in the limit of vanishing impurity concentration and zero temperature. We show that the linewidth of the down-going impurity mode ($\nu < 1.507$ THz) can be quantitatively accounted for by the decay into a single acoustic phonon, whereas that of the up-going mode above 1.93 THz is due mainly to decay into a phonon-magnon pair.

I. INTRODUCTION

In FeF_2:Mn, an S_0-symmetry local magnon (totally symmetric under the local crystal-group operations) exists just below the host spin-wave band.[1] In the absence of an external magnetic field and in the limit of very small impurity concentration the local modes associated with the impurities in the up and the down sublattices are degenerate, with frequency 1.507 THz (50.27 cm^{-1}). The magnon bands extend from 1.575 to 2.35 THz (52.54 to 78.39 cm^{-1}) at zero field. When a magnetic field is applied along the symmetry axis, the degeneracy is lifted: The frequency of the local mode decreases or increases with increasing field, depending on whether the associated impurity spin lies on the sublattice with spin dominantly parallel or antiparallel to the field. We will refer to them as the "down-going" and "up-going" modes, respectively.

These local modes have recently been investigated in detail experimentally with high-resolution far-infrared laser spectroscopy.[1-3] Because of the proximity of their energy to the magnon band edge, the wave function of these local modes is spatially extended around the Mn impurity so that there is substantial participation of the host Fe spins in the excitation. Experimentally observed consequences include the "frequency pulling" of the host and impurity modes and the large enhancement of the impurity-mode intensity in far-infrared absorption[1] and Raman scattering.[4] One of the most interesting aspects of the dynamics of these modes is the manner by which they relax their energy to the lattice. The experimental linewidth varies strongly with the impurity concentration and thickness of the disk-shaped samples, as well as with temperature. The thickness-dependent contribution has been shown to arise from radiation damping.[1-3] The concentration dependence is due to the impurity-impurity interaction,[5] which, because of the large spatial extent of the modes, contributes to line broadening even at impurity concentrations as low as 10^{-5}. More interesting yet is the fact that the linewidth extrapolated to zero impurity concentration, zero thickness, and zero temperature is greater than 1 kOe and changes with frequency, whereas the residual intrinsic linewidth of the $k=0$ magnon is only of the order of 30 Oe.[3]

For the up-going local mode the only published experiment[1] measures the linewidth at a field where this mode is degenerate with the down-going magnon continuum. Anisotropy and dipolar interactions which break the spin-rotational symmetry about the field axis provide a mechanism for decay of the local modes into band magnons, but calculation[6] suggests that less than half of the observed width can be explained in this way. More obviously for the down-going local mode, which is energetically the lowest-lying magnetic excitation in the system, the large residual width implies important interaction with, and decay into, nonmagnetic excitations, almost certainly phonons. It is this phenomenon to which the present paper is devoted. The qualitative suggestion of a phonon decay mechanism to explain the residual local-mode linewidth has been made in print by Motokawa[7] and has been alluded to elsewhere,[6] but the behavior we predict below is both more complex and more interesting than had previously been envisioned.

In this paper we investigate several local-mode decay processes involving phonons that might contribute to the residual impurity linewidth in FeF_2:Mn. At least two arguments suggest that phonons play an important role in the damping of the local mode: Acoustic phonons are the only collective excitations in FeF_2 with energies below the Mn impurity mode, and the magnetic moments ("spins") of the Fe^{2+} ions that participate in the local-mode excita-

tion couple strongly to lattice vibrations. In pure FeF_2 phonons do not contribute to the relaxation of magnons[8] because their dispersion relations are very different; thus energy and momentum cannot be conserved simultaneously. But in Mn-doped FeF_2 there is no translational symmetry around the impurities, and the requirement of momentum conservation is relaxed.

The coupling between spins and lattice vibrations arises from several sources, the most important of which are the phonon modulation of the crystal field and the modulation of the exchange integral. Regardless of its origin, the spin-lattice interaction energy can be well described by the lowest-order terms in its expansion in lattice displacements (or phonon coordinates), with phenomenological constants. In crystals with inversion symmetry, in the continuum limit, the lowest-order term of the interaction energy between a spin $\vec{S}$ and the lattice displacement $\vec{u}$ can be written[9] as

$$\mathscr{H}_{\mathrm{SL}} \simeq b_{\alpha\beta\gamma\delta} S^{\alpha} S^{\beta} \frac{\partial u_{\gamma}}{\partial x_{\delta}} , \tag{1.1}$$

where the $b_{\alpha\beta\gamma\delta}$ are the magnetoelastic coupling coefficients and the Greek subscripts and superscripts label the three Cartesian directions. The terms in S^xS^z and S^yS^z give rise to one-magnon—one-phonon decay, whereas those in S^xS^y, S^zS^z, etc., give rise to two-magnon—one-phonon decay processes. The former terms are also responsible for the coupling between propagating magnons and phonons that produce hybrid magnetoelastic modes. These modes have been extensively studied in ferromagnets with microwave resonance and ultrasonic techniques.[10] In FeF_2 the dispersion relations of the magnetoelastic excitations have been measured over the entire Brillouin zone with inelastic neutron scattering.[11] From these measurements one can obtain values of suitable components of the magnetoelastic coupling tensor b, and thereby an estimate of the decay of the local mode into acoustic phonons. Such an estimate suggests that this mechanism might indeed contribute substantially to the observed linewidth. Here, however, we will go back to the spin-lattice interaction Hamiltonian ($\mathscr{H}_{\mathrm{SL}}$) derived by Lovesey[12] from first-principles. This will give us the extra flexibility to calculate the interaction between magnons and optical phonons, and to explore the corresponding additional relaxation channels. As shown by Lovesey, the dominant mechanism for the interaction between the spins of the Fe^{2+} ions and the lattice vibrations is the modulation of the crystal field. Since the Mn^{2+} impurity has an orbital S-symmetry ground state, the spin couples negligibly to the lattice. This results in a much smaller magnetoelastic coupling in MnF_2 (Ref. 13) ($b \sim 2\times10^{-16}$ erg) than in FeF_2 ($b \sim 6\times10^{-15}$ erg). Therefore, for the local-mode—phonon decay processes to be significant, the participation of the Fe^{2+} neighbors in the impurity mode is essential.

In Sec. II we derive the Hamiltonian for calculation of the relaxation rates. This includes a magnetic part, appropriate for the impurity-mode problem, a phonon part, and the various possible magnon-phonon interaction terms. In Sec. III the contributions of the various phonon-assisted processes to the linewidth of the local magnon mode are calculated. In Sec. IV we evaluate the linewidth for the FeF_2:Mn system and compare the result with the existing data.

II. HAMILTONIAN

The system of coupled magnons and phonons is conveniently described by a Hamiltonian separated as

$$\mathscr{H} = \mathscr{H}_{\mathrm{mag}} + \mathscr{H}_{\mathrm{ph}} + \mathscr{H}_{\mathrm{int}} , \tag{2.1}$$

with independent magnons and phonons represented by the first two terms; the remaining small magnon-phonon interaction can be treated perturbatively.

A. Magnons

The rigid-lattice magnetic Hamiltonian is taken to include isotropic exchange, single-ion uniaxial anisotropy along the c axis of the lattice (chosen here as the z direction), and the Zeeman interaction with a magnetic field H_0 applied also along the c axis,

$$\mathscr{H}_{\mathrm{mag}} = \mu_B H_0 \sum_l g_l S_l^z + 2J \sum_{l,\delta} \vec{S}_l \cdot \vec{S}_{l+\delta} - D \sum_l (S_l^z)^2 + 2J_2' \vec{S}_0 \cdot \sum_{\delta_2} \vec{S}_{\delta_2} - 2J_1' \vec{S}_0 \cdot \sum_{\delta_1} \vec{S}_{\delta_1} - D'(S_0^z)^2 , \tag{2.2}$$

where sites are labeled by subscripts on the spin operators and a single impurity is located at the origin ($l=0$). We have retained only the dominant exchange terms, between next-nearest neighbors on opposite sublattices of the body-centered tetragonal arrangement of magnetic atoms, for the pure-FeF_2 host or between Fe spins. The impurity spin is taken to couple with its eight next-nearest neighbors at positions δ_2, and its two nearest neighbors at positions δ_1. This approximate exchange Hamiltonian is known[14] to give a satisfactory description of the magnon spectrum. Additional small terms which break rotational symmetries, notably the dipolar and orthorhombic anisotropy interactions which relax total S_z conservation, can be important sources of magnon decay processes even though they have little effect on the spectrum. Their contribution to the local-mode linewidth has been analyzed elsewhere[6] and should be added to the contribution calculated here.

The approximate diagonalization of (2.2) as a sum of independent (unrenormalized) magnon contributions is accomplished by a transformation to boson operators,

$$c_{\alpha} = \sum_l \Gamma_l^{\alpha} S_l^{\pm} / (2S_l)^{1/2} , \tag{2.3}$$

where the normalization has been chosen so that

$$\sum_i \Gamma_i^{\lambda} \Gamma_i^{\nu *} - \sum_j \Gamma_j^{\lambda} \Gamma_j^{\nu *} = \pm \delta_{\lambda\nu} , \tag{2.4}$$

with i summed over sites on the "up" and j over those on the "down" sublattice. The positive sign on the right-hand side [and S^+ operators in (2.3)] holds for modes whose energy increases with increasing field (up-going magnon branch) and the negative sign [and S^- operators

in (2.3)] for the down-going branch. For the pure crystal these are the usual[8] plane-wave solutions,

$$\Gamma_i^\lambda = N^{-1/2} u_k e^{-i\vec{k}\cdot\vec{r}_i}, \quad \Gamma_j^\lambda = N^{-1/2} v_k e^{-i\vec{k}\cdot\vec{r}_j}, \tag{2.5}$$

where N is the number of sites per sublattice; the coefficients v_k and $u_k = (v_k^2+1)^{1/2}$ determine the relative spin-deviation amplitudes on the two sublattices. The mode index λ in this case labels wave vector $\vec{k}$ and branch [up-going or down-going; the relation (2.5) has been written explicitly for the up-going branch]. The diagonalization is complete only insofar as higher than quadratic terms in the spin-deviation or boson operators are neglected, a useful approximation in the low-temperature limit to which we restrict ourselves. We define the corresponding quadratic boson Hamiltonian for the pure- (with full crystal translational symmetry) FeF_2 system as $\mathscr{H}_0$ and that for the impure system (with a single substitutional Mn impurity at the origin) as $\mathscr{H} \equiv \mathscr{H}_0 + V$,

$$\mathscr{H} \equiv \sum_{l,m} \mathscr{H}_{lm} b_l^\dagger b_m = \sum_\alpha \epsilon_\alpha c_\alpha^\dagger c_\alpha, \tag{2.6}$$

where we have defined a representation labeled by site indices, with b_l a suitably defined boson annihilation operator at site l. The equation of motion for c_α then gives

$$\sum_{l,m} (\epsilon_\alpha \delta_{lm} - \mathscr{H}_{lm}) \Gamma_m^\alpha = 0, \tag{2.7}$$

which can be solved for both eigenfrequencies ϵ_α and eigenfunctions Γ^α in terms of the solution to the pure-crystal problem in a familiar way—by taking advantage of the spatial locality of the impurity perturbation V, and rewriting Eq. (2.7) as

$$\Gamma^\alpha = G_0(\epsilon_\alpha) V \Gamma^\alpha, \tag{2.8}$$

where $G_0(\omega) \equiv (\omega - \mathscr{H}_0)^{-1}$ is the pure-crystal Green's function in the quadratic-boson-Hamiltonian approximation. The properties of $G_0(\omega)$ are well known, and the elements for small separation of its spatial indices have been numerically tabulated.[15] The right-hand side of Eq. (2.8) involves only those Γ_l's at the few sites l for which the localized perturbation V_{ml} is nonzero; thus (2.8) gives a small set of coupled linear homogeneous algebraic equations for those Γ_l's (and the eigenvalues ϵ_α). Then the right-hand side of Eq. (2.8) is determined, and Γ_m^α at an arbitrary site m is given directly by that equation.

In particular, the energy just below the magnon-band minimum and the wave function of the S_0 local mode associated with the Mn^{2+} impurity in FeF_2 have been studied in detail.[16] We have already pointed out that the local-mode wave function spreads over many host Fe^{2+} spins. This is evident in the greatly enhanced response of the impurity mode to long-wavelength external probes, such as in far-infrared-absorption and Raman scattering experiments. Since the spins of the Fe^{2+} ions couple strongly to lattice vibrations, whereas the orbital S-state Mn^{2+} ion does not, the substantial participation of the neighbors of the Mn impurity in the local mode also provides spin-lattice relaxation channels for the impurity mode. The coupling between the local mode and the lattice is thus expected to change with the intensity of the field H_0, since the g factor of the Mn impurity (2.0) is different from that of the host Fe ions (2.23), and the spatial extent of the local mode is highly sensitive to its separation in energy from the band minimum.

B. Phonons

The lattice vibrational modes are, of course, also affected by the impurity. However, the substitution of one doubly charged $3d$ ion (Fe^{2+}) by its equally charged neighbor in the Periodic Table (Mn^{2+}) has little effect on either the masses or force constants in the dynamical matrices. There will certainly be no highly localized phonons with energies outside the bands, and we can safely neglect the deviations from plane waves of the wave functions appropriate to the pure crystal. Thus the phonons will be characterized by wave vector $\vec{q}$ and band index μ, with the phonon Hamiltonian

$$\mathscr{H} = \sum_{\vec{q},\mu} \hbar\omega_{\vec{q}\mu} (a_{\vec{q}\mu}^\dagger a_{\vec{q}\mu} + \tfrac{1}{2}). \tag{2.9}$$

The boson operators a and $a^\dagger$ are related to the atomic displacement $\vec{u}$ by

$$\vec{u}_{l,i}(\vec{q},\mu) = \exp(i\vec{q}\cdot\vec{r}_{li}) \vec{e}_i(\vec{q},\mu) \times (\hbar/2NM_i\omega_{\vec{q}\mu})^{1/2} (a_{\vec{q}\mu} + a_{-\vec{q}\mu}^\dagger), \tag{2.10}$$

where l labels the unit cell and i the position within that cell, M_i is the mass of the ion at site i, and $\vec{e}$ is a normalized polarization vector:

$$\sum_i \vec{e}_i^*(\vec{q},\mu)\cdot\vec{e}_i(\vec{q}',\mu') = \delta_{\vec{q},\vec{q}'}\delta_{\mu\mu'}. \tag{2.11}$$

C. Magnon-phonon interaction

The spin-lattice interaction in FeF_2 was studied in detail by Lovesey,[12] who showed that the dominant mechanism is phonon modulation of the crystal field. This dominance over alternative mechanisms, such as phonon modulation of exchange fields, is confirmed by the fact that the theory neglecting all other effects accounts very accurately for the neutron-inelastic-scattering data[11] on hybrid magnon-phonon excitations in FeF_2. Since the low-lying crystal-field states in this material are well understood, the magnon-phonon coupling can be reliably calculated from first principles. Similar calculations have been made for $FeCl_2 \cdot 2H_2O$, giving quantitative agreement with the experimental data for that system.[17,18]

To second order in the spin-orbit interaction for Fe^{2+}, the effective spin-lattice interaction Hamiltonian is of the form of Eq. (1.1), with the coefficients $b_{\alpha\beta\gamma\delta}$ proportional to the square of the spin-orbit coupling constant, the inverse of each of two crystal-field energy-level splittings, and matrix elements of the crystal-field (Coulomb) interaction expanded in lattice displacement or phonon coordinates. To lowest nonvanishing order, the latter involves terms linear in the displacements, and therefore creation or destruction of a single phonon [as in Eq. (1.1)]. All the relevant parameters are well known for FeF_2.

The Coulomb matrix elements begin with an interaction with the quadrupole moment in the multipole expansion, and the one-phonon terms fall off at least as fast as the inverse fourth power of the distance of the source from the Fe^{2+} ion in question. Therefore, it is sufficient to consider the effects of only the six F^- ions nearest the Fe site, and the small distortion of their configuration from a regular octahedron can be neglected.[12] For acoustic phonons the polarization vector at such a F^- site, at position $\vec{\delta}$ relative to the Fe, is

$$\vec{e}_{\vec{\delta}}(\vec{q},\mu)=\exp(i\vec{q}\cdot\vec{\delta})(M_F/M)^{1/2}\hat{e}(\vec{q},\mu)\ , \tag{2.12}$$

where M_F is the F^- mass, M is the total mass of a unit cell, and $\hat{e}(\vec{q},\mu)$ is a unit polarization vector for the acoustic branch labeled by μ. The wave vectors of importance will be sufficiently small ($q \lesssim 0.4$ Å^{-1}) that $|q\delta| \ll 1$ (the F^- distance δ is 2.1 Å), and the phase factor in (2.12) can be approximated as $1+i\vec{q}\cdot\vec{\delta}$. Then the one-magnon—acoustic-phonon interaction Hamiltonian takes the form

$$\mathscr{H}_{\rm int}(\text{ac phonon})=-ib(\hbar S^3/MN)^{1/2}\sum_{\vec{q},\mu,\lambda}\omega_{\vec{q}\mu}^{-1/2}\left[\sum_{i\neq 0}e^{-i\vec{q}\cdot\vec{r}_i}\Gamma_i^{\lambda *}[q_z(e_{\mu x}-ite_{\mu y})+e_{\mu z}(q_x-itq_y)]\right.$$
$$\left.+\sum_j e^{-i\vec{q}\cdot\vec{r}_j}\Gamma_j^{\lambda *}[q_z(te_{\mu x}-ie_{\mu y})+e_{\mu z}(tq_x-iq_y)]\right]a_{\vec{q}\mu}^{\dagger}c_\lambda+\text{H.c.}\ , \tag{2.13}$$

where the magnetoelastic coupling constant

$$b=\frac{\lambda^2(2S-1)P\delta}{\sqrt{2}\Delta_{xy}\Delta_{xz}S}\ , \tag{2.14}$$

defined in analogy with the coefficients $b_{\alpha\beta\gamma\delta}$ of Eq. (1.1), is expressed explicitly in terms of the spin-orbit coupling constant λ, and the Coulomb matrix element P and crystal-field splittings Δ_{xy} and Δ_{xz} defined in Ref. 12. The coefficient t in Eq. (2.13) is the ratio $t\equiv R/P\simeq 0.4$, where R is a second Coulomb matrix element defined and evaluated in Ref. 12. We have used the notation $e_{\mu x}$ for the x component of the unit polarization vector $\hat{e}(\vec{q},\mu)$. The sum over the three acoustic branches is complicated. However, the calculations of Refs. 12 and 19 suggest that the $\vec{q}$ dependence of $\hat{e}(\vec{q},\mu)$ is unimportant. We also note that insofar as the three acoustic modes for given $\vec{q}$ can be characterized as longitudinal and transverse, there is no coupling to the longitudinal mode [no terms of the form $q_\alpha e_{\mu\alpha}$ in Eq. (2.13)]. Thus we expect little quantitative error from the substantial simplification of replacing the sums over modes μ of the μ-dependent factors in Eq. (2.13) by $q/(\omega_q)^{1/2}$ where ω_q is a suitable representative acoustic frequency (the "transverse"-acoustic frequency, insofar as that can be defined). Then

$$\mathscr{H}_{\rm int}(\text{ac phonon})=-i(\hbar S^3/MN)^{1/2}\times b\sum_{q,\lambda}[q/(\omega_q)^{1/2}]F_\lambda(q)a_q^{\dagger}c_\lambda+\text{H.c.}\ , \tag{2.15}$$

where the form factor $F^\lambda(q)$ is defined as

$$F^\lambda(q)\equiv\sum_{l\neq 0}e^{-i\vec{q}\cdot\vec{r}_l}\Gamma_l^{\lambda *}\ , \tag{2.16}$$

essentially the Fourier transform of the magnon wave function at the phonon wave vector. As one would expect, this simply measures the extent of spatial matching of the two excitations, excluding the impurity spin at the origin $l=0$, which does not couple to the phonon field. For $\lambda=0$, corresponding to the local (S_0-symmetry) magnon, from Eq. (2.8) and the explicit form of the pure-crystal Green's function,[16] we have

$$F^0(q)=\omega_E[(A_0+2A_1)(\omega^+ +\gamma_q)+8A_2(\omega^- -\gamma_q)]/[(\omega_L+\omega_H)^2-\omega_q^2]-\Gamma_0\ , \tag{2.17}$$

where ω_L is the local magnon energy, $\omega_E=16JS$ is the exchange energy, $\omega_H=g\mu_B H_0$ is the Zeeman energy, $\omega^\pm=(\omega_L+\omega_H\pm\omega_E\pm\omega_A)/\omega_E$ with $\omega_A=(2S-1)D$ the anisotropy energy, and $8\gamma_q=\sum_{\vec{\delta}}\exp(i\vec{q}\cdot\vec{\delta})$ with $\vec{\delta}$ summed over lattice vectors from a magnetic site to nearest magnetic neighbors on the opposite sublattice (i.e., to next-nearest magnetic neighbors). The three numbers A_0, A_1, and A_2 are essentially the local-mode amplitudes,

$$A_l=\sum_m V_{lm}\Gamma_m\ , \tag{2.18}$$

where A_0 refers to $l=0$ (the impurity site), A_1 to $l=\delta_1$ (a nearest-neighbor site), and A_2 to $l=\delta_2$ (a next-nearest-neighbor site). For the S-symmetry mode the value of A_2 is, by definition, independent of which of the eight next-nearest neighbors is chosen; similarly A_1 does not refer to a particular near neighbor. The values of the A_l are given in Ref. 16. For $H_0<0$ the result (2.17) refers to the upgoing local mode, and for $H_0>0$ it refers to the downgoing mode.

Of the various optical-phonon branches only that with B_{1g} symmetry at $q=0$ lies low enough to fall within the

frequency range of interest here: At $q=0$ its frequency is 2.04 THz (68 cm^{-1}); thus this branch can provide a channel for single-phonon decay of the up-going local magnon at reasonable magnetic fields. In general, at small q the relative motion of atoms within a unit cell is larger for an optical than for an acoustic phonon, and one would anticipate a relatively strong magnon-phonon coupling. That expectation is mitigated somewhat in this particular case where at $q=0$ only the F^- ions move, and their displacements are perpendicular to the line joining them to the nearest magnetic ion.[19,20] Of course, this is also the reason that the corresponding optical-phonon frequency is relatively low. Nevertheless, this is a potentially important decay mechanism. Using the proper normal coordinates and assuming $q\delta \ll 1$, we can sum the body-centered and corner-site interactions over all sites except $i=0$ to find

$$\mathscr{H}_{\rm int}(B_{1g})=\left[\frac{\hbar S^3 t\delta}{8NM_{\rm F}}\right]^{1/2} b\sum_{q,\lambda} q^2\omega_q^{-1/2}B^{\lambda}(q)a_q^{\dagger}c_{\lambda}+\text{H.c.}\ , \tag{2.19}$$

where the coupling parameter now is given by

$$q^2B^{\lambda}(q)=iF_i^{\lambda}(q)q_xq_z+F_j^{\lambda}(q)q_yq_z\ , \tag{2.20}$$

with

$$\begin{aligned}F_i^{\lambda}(q)&=\omega_E[(A_0+2A_1)\omega^+\\&\quad -8A_2\gamma_q]/[(\omega_L+\omega_H)^2-\omega_q^2]-\Gamma_0\ ,\\ F_j^{\lambda}(q)&=\omega_E[(A_0+2A_1)\gamma_q+8A_2\omega^-]/[\omega_L+\omega_H)^2-\omega_q^2]\ .\end{aligned} \tag{2.21}$$

The terms in S^xS^y, $(S^x)^2$, and $(S^z)^2$ in the spin-lattice Hamiltonian give rise to processes in which the local magnon mode decays into one phonon and one propagating magnon. However, contrary to the situation for the one-magnon interaction described by (2.13), in general acoustic phonons of all polarizations are coupled to two magnons of arbitrary wave vectors. The interaction Hamiltonian is now lengthy, since there are three different magnetoelastic coupling coefficients, and each one multiplies a different combination of products of momentum and polarization vectors of the type that appear in (2.13). But since the energies of the two excited crystal-field states are not much different, and $t\simeq 0.4$, the three coupling coefficients are nearly the same. Assuming they are all equal and using the same type of approximations as before we obtain, for the up-going impurity mode,

$$\mathscr{H}_{\rm int}(\text{mag}+\text{ac phonon})\simeq\left[\frac{2\hbar S^2}{N^2M}\right]^{1/2} b\sum_{\substack{\vec{q},\vec{k},\\ \lambda,\mu}} q\omega_{q\mu}^{-1/2}[v_kF_i^{\lambda}(\vec{q}+\vec{k})+u_kF_j^{\lambda}(\vec{q}+\vec{k})]a_{q\mu}^{\dagger}c_k^{\dagger}c_{\lambda}+\text{H.c.}\ , \tag{2.22}$$

where μ now labels the acoustic-phonon branch. For the down-going impurity mode the interaction takes exactly the same form, but with u_k and v_k interchanged.

III. LINEWIDTH CALCULATION

The simplest process for local-magnon relaxation is direct decay into a single phonon. In the absence of crystalline translational symmetry (because of the impurity), the requirements of wave-vector conservation are relaxed. In general, the local magnon can decay into any phonon energetically degenerate with it (unless other symmetries prevent magnon-phonon coupling), as illustrated in Fig. 1. In FeF_2 the transverse-acoustic phonon bands extend as high as 3 THz, and above 2.04 THz the magnon also becomes degenerate with phonons in the B_{1g} optical band. At temperatures low compared with the local-magnon energy, where the number of thermally excited phonons degenerate with that magnon is negligible, the standard golden-rule expression for the decay rate of the local mode into a single phonon from the branch labeled by μ gives the linewidth contribution

$$\Delta H_{\mu}=\frac{2\pi}{\gamma\hbar^2}\sum_{\vec{q}}|V_{\vec{q}\mu}|^2\delta(\omega_L-\omega_{q\mu})\ , \tag{3.1}$$

where $V_{\vec{q}\mu}$ is the matrix element of the interaction Hamiltonian between the states of a single-local-magnon excitation and excitations of a single phonon of wave vector $\vec{q}$

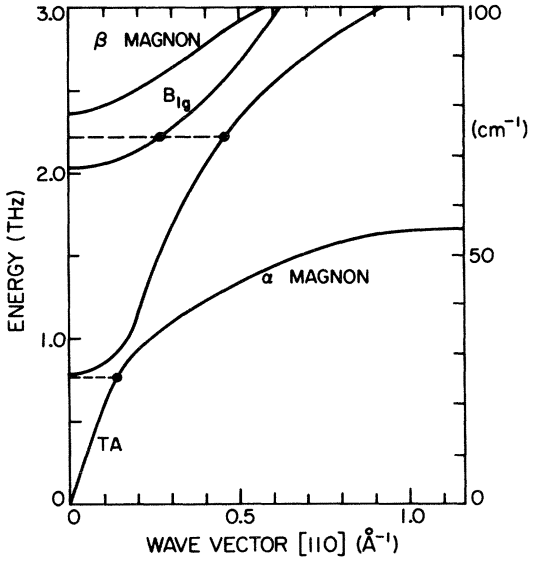

FIG. 1. Dispersion relations for low-lying phonons and both magnon branches in a magnetic field for FeF_2:Mn. The local-mode energies (on both sublattices) are indicated as dashed lines; their potential decay into a single acoustic (TA) or optical (B_{1g}) phonon or into a down-going magnon is indicated by the solid circles.

on branch μ. For $\vec{q}$ along the high-symmetry directions [100] or [110] in FeF_2, the matrix elements $V_{\vec{q}\mu}$ vanish for the longitudinal- and one of the two transverse-acoustic branches. Although the situation is more complicated in a general direction of $\vec{q}$ we approximate the sum over μ in (3.1) by assuming an effective contribution from a single branch. The phonon dispersion relation can be approximated by the isotropic analytic expression

$$\omega(q)\simeq c_0 q - c_1 q^3 , \tag{3.2}$$

where the values $c_0=19.6$ meV Å and $c_1=3.94$ meV Å^3 reproduce[12] the experimental dispersion curve accurately for $\vec{q}$ in the [100] direction and represent a good approximation for the transverse phonons in all directions. Within this approximation the linewidth contribution (2.15) from decay into single transverse-acoustic phonons becomes

$$\Delta H_{\rm TA}\simeq\frac{S^3b^2}{\pi\gamma\hbar\rho}\int dq\frac{q^4}{\omega_q}|F(q)|^2\delta(\omega_L-\omega_q)$$
$$=\frac{S^3b^2}{\pi\gamma\hbar\rho}\frac{q_0^4|F(q_0)|^2}{\omega_L(c_0-3c_1q_0^2)} , \tag{3.3}$$

where ρ is the mass density, the form factor $F(q)$ is given by Eq. (2.17), and q_0 is the wave number of the phonons degenerate with the local magnon, $\omega(q_0)=\omega_L$. The phonon density of states, characterized by the denominator $(c_0-3c_1q_0^2)^{-1}$, is the important feature of the acoustic-phonon spectrum affecting the linewidth. The smooth, monotonically increasing function of our approximation is a reasonable representation of the actual density of states.

For the B_{1g} optical phonon we use the interaction Hamiltonian (2.19) and assume an isotropic dispersion relation of the form

$$\omega(q)=\omega_0+aq^2 \tag{3.4}$$

The zone-center minimum energy ω_0 has been determined at $T=10$ K by Raman scattering[4] to be 2.06 THz. Since the full dispersion relation for FeF_2 has not been experimentally determined, we assume it to be similar to the isomorphic antiferromagnetic crystal MnF_2, with very similar lattice parameters and ionic masses. The phonon dispersion relations for MnF_2 are well known,[21] and in MnF_2 the coefficient a in (3.4) is $a\simeq 2.5$ THz Å^2. Then we find for this contribution to the linewidth

$$\Delta H(B_{1g})\simeq\frac{S^3(bt\delta)^2}{60\pi\gamma\hbar a\rho}\left[\frac{M}{4M_{\rm F}}\right]\frac{q_0^5|\tilde{F}(q_0)|^2}{\omega_L} , \tag{3.5}$$

where the effective form factor is

$$|\tilde{F}(q_0)|^2\equiv F_i^2(q_0)+F_j^2(q_0) , \tag{3.6}$$

i.e., the sum of the corresponding factors for the two sublattices.

Between 1.54 and 1.93 THz the up-going local mode is degenerate with the down-going magnon continuum, but decay into this continuum is strongly inhibited by total S_z conservation. The relaxation of this requirement by the small symmetry-breaking terms of the magnetic Hamiltonian (dipolar and orthorhombic anisotropy interactions) has been calculated in Ref. 6; it seems to explain only a fraction of the observed linewidth. But the magnon-phonon coupling also provides a mechanism for opening this decay channel. The down-going "magnon" excitations are more properly coupled magnetoelastic modes, and though the phonon admixture is small, except near the point where the magnon and acoustic-phonon dispersion curves cross, it does also allow direct decay of the local magnon to these modes, as illustrated in Fig. 2. In fact the crossing of the magnon and phonon dispersion curves occurs right in the region of interest, at an energy of about 1.75 THz at a magnetic field such that the up-going local mode also has this energy. Nevertheless, the effect of this magnetoelastic mixing on the linewidth turns out to be small. The calculation is straightforward, starting from the pure-crystal magnetoelastic Hamiltonian,

$$\mathcal{H}_{0\alpha}(\text{mag-el})=\sum_k\hbar\epsilon_{k\alpha}c_{k\alpha}^\dagger c_{k\alpha}+\sum_q\hbar\omega_q a_q^\dagger a_q$$
$$+(i\hbar/2)\sum_k\sigma_k c_{k\alpha}^\dagger a_k+\text{H.c.} , \tag{3.7}$$

where we have again simplified the calculation to a single effective phonon mode and have written only the part appropriate to one of the two magnon branches, here labeled by α. The magnetoelastic coupling constant σ_k for the down-going magnon is given by[22]

$$\sigma_k=\left[\frac{4b^2S^3}{\hbar\omega_k M}\right]^{1/2}(u_k+v_k)k \tag{3.8}$$

within the approximation that the band-magnon wave functions are given adequately by plane waves (in fact they must be distorted precisely in the neighborhood of the impurity so as to be orthogonal to the local mode, but it is very difficult to account for that explicitly).

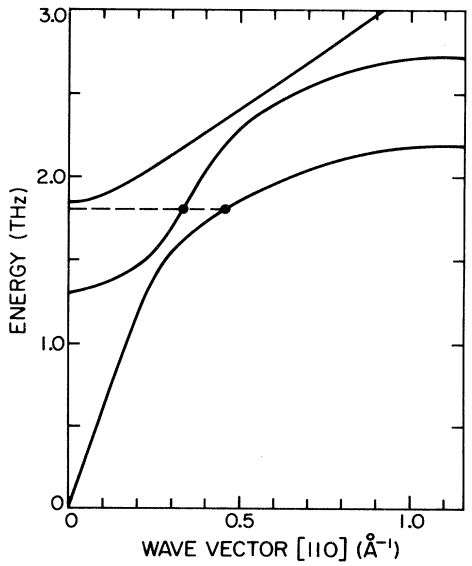

FIG. 2. Potential decay path for the up-going local mode into a single spatially extended excitation, as in Fig. 1, but for a field such that this final-state excitation is a strongly mixed magnetoelastic mode.

The Hamiltonian (3.7) is quadratic in boson operators and therefore readily diagonalized by a canonical Bogoliubov transformation[23]

$$c_k = x_k b_{k+} + z_k b_{k-} , \quad a_k = z_k b_{k+} + x_k b_{k-} , \tag{3.9}$$

with $x_k^2 + z_k^2 = 1$ to preserve the commutation relations. The calculation of the decay of a local magnon into the magnetoelastic modes created by $b_{k\pm}^\dagger$ goes through just as before [with the result (3.3) for the linewidth] except that the effective coupling b^2 will contain an extra multiplicative factor x_k^2 or z_k^2 reflecting the phonon admixture in this magnetoelastic excitation, and the density of states will be that of those mixed excitations. In general (see Fig. 2), the local-mode frequency intersects both magnetoelastic branches. If the local magnon is well above the crossover energy, where uncoupled magnon and acoustic-phonon dispersion curves cross, as sketched in Fig. 2, then the decay mode on the upper branch (created by $b_{k+}^\dagger$) is primarily a phonon, the admixture factor z_k^2 is close to unity, and the density of states is nearly that of acoustic phonons. The earlier results, in other words, are only slightly modified. The new channel is provided by the crossing of the lower magnetoelastic branch, which is largely of magnon character. The coupling is modified by the mixing factor

$$x_k^2 = \frac{1}{2} - \frac{1}{2}\left[1 + \left[\frac{\sigma_k}{\omega_k - \epsilon_{k\alpha}}\right]^2\right]^{-1/2} \approx \frac{\sigma_k^2}{4(\omega_k - \epsilon_{k\alpha})^2} , \tag{3.10}$$

which is small compared to unity in the region of interest, but the density of states is essentially that of magnons, which becomes large near the zone boundary. However, we will find below that this contribution does not become numerically important in this region. One might expect the magnetoelastic coupling to lead to substantial alterations in the linewidth for local-mode energies near E_x, the magnon-phonon crossover energy. In fact, this is not the case. A standard, nearly degenerate perturbation-theory calculation at precisely that energy gives solutions at wave vectors $q - q_x = \pm\sigma_x (c_0 c_m)^{-1/2}$, where again the subscript "x" denotes the crossover points, and c_0 and c_m are the group velocities of bare phonon and magnon at that point. Factors in the linewidth involving analytic functions of q, including u_q, v_q, and the form factors, are given by their values at the crossover plus *second*-order corrections in $|q - q_x|$ when summed over the two solutions symmetrically located in $q - q_x$ (as first-order corrections cancel). There remain the factors $z_q^2 \simeq c_m/(c_0 + c_m)$, measuring the phonon admixture, and the density of states, proportional to $(dE/dq)^{-1}$, appropriate to the new mixed magnetoelastic modes with energies $E(q)$,

$$\frac{z_q^2}{dE/dq} \simeq \left[\frac{c_m}{c_0 + c_m}\right]\left[\frac{c_0 + c_m}{2c_m c_0}\right] = \frac{1}{2c_0} , \tag{3.11}$$

for *each* of the two modes, so that through first order in $|q - q_x|$ the contribution to the linewidth is the same as from the original bare phonon, with $z_q^2 \to 1$ and $dE/dq = c_0$ (note half the contribution comes from each of the magnetoelastic modes at energy E_x). Numerical calculations bear this out; the bare-phonon contributions to the local-mode linewidth are altered by less than 1% when the proper coupled magnetoelastic modes are used.

Finally, we consider the local-mode linewidth contributions due to decay into a magnon plus an acoustic phonon, described by the interaction Hamiltonian (2.22). For reasons of energy conservation this mechanism applies only above a local-mode threshold energy of 1.54 THz (i.e., only for the up-going local mode and at fields $H_0 > 11$ kOe). Again the magnetoelastic modes should really be considered, but with energy conservation now restricting only the *sum* of magnon and phonon energies in the final state, these excitations can be located over much of the Brillouin zone for any given local-mode energy. In general, they are well removed from the crossover region, and the admixture effects are less important than before. Because of the magnon energy gap, for fields (and local-mode energies) of interest here, the majority of the energy goes into the final magnon, and the low-energy final phonons are adequately described by the linear dispersion relation $\omega_\mu(q) = c_{0\mu} q$ for the acoustic branch labeled by μ. If we neglect the wave-vector anisotropy in the dispersion relations $\omega_\mu(q)$ for phonons and $\epsilon(k)$ for down-going magnons, then the golden-rule expression for the linewidth can be readily written as an integral over the final magnon momentum $\vec{k}$ only,

$$\Delta H(\text{mag} + \text{phonon}) \simeq \frac{S^2 b^2 \Omega}{4\pi^4 \gamma \hbar \rho} \times \int d^3k \, q_0^3(k) \, |C(\vec{k}, \vec{q}_0)|^2 / c_{0\mu}^2 , \tag{3.12}$$

where $q_0(k)$ is the phonon wave vector demanded by energy conservation: $\omega_\mu(q_0) = \omega_L - \epsilon(k)$, and the effective form factor is

$$C(\vec{k}, \vec{q}_0) = v_k F_i(\vec{k} + \vec{q}_0) + u_k F_j(\vec{k} + \vec{q}_0) . \tag{3.13}$$

In doing the integral over $\vec{q}$ to arrive at the result (3.12), we have neglected the weak dependence of F_i and F_j on the direction of their argument, $\vec{k} + \vec{q}_0$.

IV. NUMERICAL RESULTS AND COMPARISON WITH EXPERIMENT

We can evaluate the magnetoelastic coupling coefficient b defined in Eq. (2.14) with the values of the parameters given by Lovesey.[12] With $\lambda = 85$ cm^{-1}, $\Delta_{xy} = 800$ cm^{-1}, $\Delta_{zy} = 1000$ cm^{-1}, $S = 2$, $\delta = 2.12$ Å, and $P = 0.004 e^2/a_0^2$, where e is the electron charge and a_0 is the Bohr radius, we obtain $b = 6.6 \times 10^{-15}$ erg. Note that this value, derived from first principles, gives a magnetoelastic splitting σ_k [defined in Eq. (3.8)], at $k_x \sim 0.4$ Å^{-1}, of 0.13 THz or 0.53 meV, which agrees very well with the experimental neutron-inelastic-scattering value of about 0.4 meV (in the [100] direction; the value is direction dependent since anisotropic dispersion relations for bare magnons and phonons lead to different crossing points for

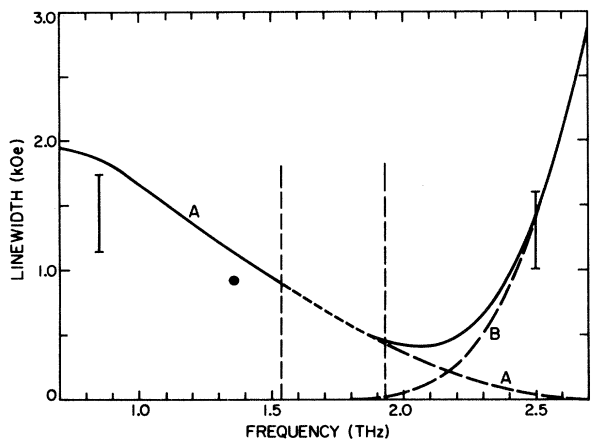

FIG. 3. Residual local-mode linewidth in FeF_2:Mn from phonon-associated relaxation processes. Theoretical curves are labeled *A* (decay to a single phonon) and *B* (decay into a phonon-magnon pair). Proper treatment of the region between 1.54 and 1.93 THz is beyond the scope of this paper (see text). Experimental error for the point of 1.36 THz is smaller than the diameter of the solid circle; the other error bars are discussed in the text.

the dispersion curves in different directions in reciprocal space). With this value of b we obtain the linewidth shown in Fig. 3 as a function of the local-mode frequency. Note that the ranges below and above 1.507 THz correspond to the down-going and the up-going local modes, respectively.

Curve *A* in Fig. 3 represents the contribution from the direct one magnon to one bare acoustic-phonon process given by Eq. (3.3). Near 1.7 THz, as we have pointed out above, the bare phonon is not a good approximation to the relevant magnetoelastic mode because there is substantial admixture of a magnon from the down-going branch, but the net effect of this admixture on the linewidth is small. Away from this region the frequency dependence of curve *A* arises from two sources: (i) the phonon density of states, essentially proportional to ω^3 since the phonon dispersion relation is almost linear over the range of frequencies of interest, and (ii) the form factor $|F(q)|^2$. The wave function[16] is roughly Yukawa shaped, $\Gamma_i \sim \exp(-\kappa r_i)/r_i$, with the characteristic size κ^{-1} of the order of a few lattice spacings. Thus $F(q) \sim (q^2+\kappa^2)^{-1}$, and for $q \gtrsim \kappa$ and $q \simeq \omega/c_0$ (c_0 is the velocity of sound) we see that $|F(q)|^2 \sim \omega^{-4}$, which dominates the density-of-states factor. Further, as the local-mode frequency increases, it is separated further from the magnon band edge, because the g factor of the Fe spin is about 10% larger than that for Mn. The impurity mode then becomes increasingly localized spatially; i.e., κ increases. The overall result is a substantial decrease of linewidth with increasing frequency.

The contribution of the B_{1g} optical phonon to the linewidth, given by Eq. (3.5), is always small. It vanishes at frequencies below 2.06 THz, rises to a maximum of about 5 Oe at 2.3 THz, and falls slightly out to the maximum frequency values of interest here ($\sim$2.7 THz). It is instructive to compare the single optical- and acoustic-phonon contributions as given by Eqs. (3.5) and (3.3), respectively. As expected, the optical process is enhanced by a relative density of states, $c_0/2aq \simeq 1/q$ (in Å^{-1}) and by comparatively large relative ionic motion, as reflected in the factor $M/4M_F \simeq 2.5$. As we mentioned above, however, the symmetry of this optical mode implies rather weak coupling, at least at small q, reflected in the extra factor of $(qd)^2$ and in the angular factors $q_x q_z/q^2$ and $q_y q_z/q^2$ of the coupling constant (2.20); the square of each gives an angular average of 1/15, an explicit factor in Eq. (3.5). The relevant Coulomb matrix element is also smaller; the factor of t^2 in (3.5) gives a reduction of approximately 0.16. The net result is a reduction from the acoustic contribution, typically of the order of 100 Oe, to a few Oe for the optical phonon over the range of interest.

We find that at high frequencies the linewidth is dominated by relaxation to a magnon—acoustic-phonon pair, as given by Eq. (3.12). Because the square of the matrix element is inversely proportional to the phonon energy and the density of states is inversely proportional to the phonon velocity, this process is dominated by the transverse-acoustic-phonon branch with the lowest energy. Along [110] this corresponds to polarization $e_x = e_y$, $e_z = 0$, and a sound velocity of $c_{0t} \simeq 2 \times 10^5$ cm/sec, the lowest for any direction of propagation. The velocity rises to a maximum of $c_{0t} \simeq 3 \times 10^5$ cm/sec along [100]. The angular integrals in Eq. (3.12) are difficult to perform, and there are no reported measurements of the phonon dispersion relation in general directions in any case, so we have replaced all angularly dependent factors in the integrand by simple averages of their maximum and minimum values. As we remarked below Eq. (3.13), we recognize that $F_i(\vec{k}+\vec{q}_0)$ and $F_j(\vec{k}+\vec{q}_0)$ depend importantly only on the absolute value of their arguments. Then the only dependence on the direction of $\vec{q}$ is in the factor $c_{0t}^{-2}(\vec{q})$, which is replaced by its average over the [100] and [110] directions. The form factor itself is then replaced by the average between $\vec{k}$ parallel and antiparallel to $\vec{q}$ (i.e., $\theta_{\vec{k},\vec{q}} = 0$ and π). The contribution to the local-mode linewidth of this process of relaxation to a magnon plus a phonon, as calculated within the approximation just described, is plotted as curve *B* in Fig. 3. The contribution becomes significant around 2 THz and increases rapidly with frequency. We indicate the behavior only up to 2.7 THz; at higher frequencies the approximation for the phonon dispersion relation is inadequate.

We have discussed above local-mode decay into magnetoelastic modes in the frequency range 1.54—1.93 THz where the up-going local mode is degenerate with the down-going magnon band. Of course, the S_z-symmetry—breaking interactions (notably orthorhombic anisotropy) discussed in Ref. 6 also provide for decay into these same final states, and we should properly take into account the quantum interference between the amplitudes for the two processes in calculating the probability for decay. Since the two mechanisms calculated independently give comparable contribution to the linewidth in the re-

gion of interest, the interference term can be of substantial importance. However, to carry out the amplitude calculation for the symmetry-breaking anisotropy interaction to find both magnitude and phase, we need the final-state wave function. The impurity offers primarily a magnetic contrast to the host atoms, and as opposed to the phonon final states we have considered above, which are well represented as plane waves, the continuum magnons are distorted from plane waves precisely in the neighborhood of the impurity where their overlap with the initial local-mode state is substantial. The Green's-function calculation of Ref. 6 does not suffer from this problem, but it also does not yield the essential information about the phase of the transition amplitudes. Therefore we have marked this region where these processes can take place with vertical lines in Fig. 3, and have included only the independent contribution to the linewidth of the phonon mechanism. We do not know whether constructive interference, a slightly larger orthorhombic anisotropy constant than estimated in Ref. 6, or a combination of these may explain the relatively large observed linewidth[1] of 3 kOe at 1.75 THz, as compared with a combined theoretical value of about 1 kOe from the two mechanisms treated independently. But we do note that a factor of 2 in the anisotropy constant or completely constructive interference would each essentially remove the discrepancy, and neither seems unreasonable.

Outside the range 1.54—1.93 THz the impurity-mode linewidth has been measured only at three frequency values. Of the data points in Fig. 3 the one at 1.36 THz is the most reliable, since the contributions from radiation-damping and impurity-banding effects could be clearly identified and the measurements were made in a highly uniform field. It is gratifying that this point agrees with the calculation within 20% considering the various simplifying assumptions that were made in the evaluation of the final result. The bars at 0.85 and 2.5 THz represent data taken at the High Field Laboratory of Osaka University.[24] The upper end of the bar represents an extrapolation of the measured absorption linewidth to zero sample thickness and impurity concentration, and the length corresponds to the estimated field nonuniformity in the sample. Since the field profile and the shape of the absorption line are difficult to measure with precision, one cannot use deconvolution techniques to extract the true linewidth, but it probably lies somewhere near the middle of the bar. So at these frequencies the predictions of the theory are also confirmed by experiments.

We emphasize that there are no adjustable parameters in the theory, so the agreement with experiment is highly satisfying. We are confident that we have identified the primary local-mode-broadening mechanisms. On the other hand, the preliminary nature of two of the measurements and the considerable experimental uncertainty still leave us short of a clear demonstration of the predicted linewidth behavior as a function of frequency. With the development of broadband sources in this frequency region, notably the free-electron laser, we look forward to definitive experimental results over the whole range of Fig. 3.

ACKNOWLEDGMENTS

We gratefully acknowledge several stimulating conversations with Professor V. Jaccarino of the University of California, Santa Barbara, and Professor M. Motokawa of Osaka University. This work was supported in part by the National Science Foundation through Grant Nos. DMR-80-08004 and DMR-80-17582. One of us (S.M.R.) acknowledges the support of Conselho Nacional de Desenvolvimento Científico e Tecnólogico (CNPq), Brazil.

[1]R. W. Sanders, V. Jaccarino, and S. M. Rezende, Solid State Commun. 28, 907 (1978); R. W. Sanders, R. M. Belanger, M. Motokawa, V. Jaccarino, and S. M. Rezende, Phys. Rev. B 23, 1190 (1981).

[2]R. W. Sanders, Ph.D. thesis, University of California, Santa Barbara, 1978.

[3]R. M. (Belanger) Toussaint, Ph.D. thesis, University of California, Santa Barbara, 1982.

[4]S. M. Rezende, C. B. de Araujo, and E. Montarroyos, Solid State Commun. 35, 627 (1980).

[5]C. Wiecko and D. Hone, J. Phys. C 13, 3883 (1980).

[6]P. Thayamballi and D. Hone, Phys. Rev. B 27, 2924 (1983).

[7]M. Motokawa, J. Magn. Magn. Mater. 31-34, 683 (1983).

[8]S. M. Rezende and R. M. White, Phys. Rev. B 14, 2939 (1976).

[9]C. Kittel, Phys. Rev. 110, 836 (1958).

[10]See, for example, S. M. Rezende and F. R. Morgenthaler, J. Appl. Phys. 40, 524 (1969); B. A. Auld, in *Applied Solid State Science,* edited by R. Wolfe (Academic, New York, 1971), Vol. 2.

[11]B. D. Rainford, J. G. Houmann, and H. J. Guggenheim, in *Neutron Inelastic Scattering* (IAEA, Vienna, 1972), p. 655.

[12]S. W. Lovesey, J. Phys. C 5, 2769 (1972).

[13]R. L. Melcher, Phys. Rev. Lett. 25, 1201 (1970).

[14]M. T. Hutchings, B. D. Rainford, and H. J. Guggenheim, J. Phys. C 3, 307 (1970).

[15]L. R. Walker, B. B. Cetlin, and D. Hone, J. Phys. Chem. Solids 30, 923 (1969).

[16]S. M. Rezende, Phys. Rev. B 27, 3032 (1983).

[17]J. B. Torrance and J. C. Slonczewski, Phys. Rev. B 5, 4648 (1972).

[18]E. N. Economou, K. L. Ngai, T. L. Reinecke, J. Ruvalds, and R. Silberglitt, Phys. Rev. B 13, 3135 (1976).

[19]J. G. Traylor, H. G. Smith, R. M. Nicklow, and M. K. Wilkinson, Phys. Rev. B 3, 3457 (1971).

[20]R. S. Katiyar, J. Phys. C 3, 1087 (1970).

[21]H. G. Smith and N. Wakabayashi, in *Dynamics of Solids and Liquids by Neutron Scattering,* edited by S. W. Lovesey and T. Springer (Springer, Berlin, 1977).

[22]I. Kimura, J. Phys. Soc. Jpn. 28, 1182 (1970).

[23]S. S. Guerreiro and S. M. Rezende, Rev. Bras. Fis. 1, 207 (1971).

[24]M. Motokawa and R. M. Toussaint (unpublished).